Electronic Supplementary Material (ESI) for Sustainable Energy & Fuels.

Supplementary Information

Production of formate from CO_2 reduction and its application in energy storage

Hang Xiang[a], Hamish Andrew Miller[b], Marco Bellini[b], Henriette Christensen[a], Keith Scott [a], Shahid Rasul[a,c], Eileen H. Yu[a] *

[a] School of Engineering, Newcastle University, Newcastle Upon Tyne, UK

[b] Istituto di Chimica dei Composti Organometallici (CNR-ICCOM), Via Madonna del Piano 10, 50019 Sesto Fiorentino, Firenze, Italy

[c] Faculty of Engineering and Environment, Northumbria University, Newcastle Upon Tyne, UK

*Corresponding author: (eileen.yu@ncl.ac.uk)

Table S1 Summary of eCO_2R studies in terms of formate production

Paper	Reactor, Membrane, Catholyte, CO_2 flow.	Catalyst/cathode	Potential		Current density *j* (mA cm^{-2})	Formate FE	Formate production	
			Cell (V)	Cathodic (V vs. RHE)			Yield per hour (mg/h)	Conc. Per hour (mM/h)
Ref. [1]	H-cell +GDE holder, 0.5M $KHCO_3$, CO_2 flow 30ml/min.	GDL and Sn-loading copper mesh (rolling press) S_{geo}: 7 cm^2	——	-0.67	Ap. -3.49	Ap. 43%	Cal. 9.01	Catholyte vol. N.G.
			——	-0.87	Ap. -13.48	Ap. 46%	Cal. 37.26	Catholyte vol. N.G.
			——	-1.07	Ap. -22.44	Ap. 78%	Cal. 105.17	Catholyte vol. N.G.
			——	-1.27	Ap. -23.85	Ap. 65%	Cal. 93.15	Catholyte vol. N.G.
			——	-1.47	Ap. -36.05	Ap. 43%	Cal. 93.15	Catholyte vol. N.G.
Ref. [2]	GDE flow cell 7ml/min 0.1M $KHCO_3$, CO_2 flow 45ml/min	Sn-GDE with thin SnOx nanolayer S_{geo}: 4 cm^2	-0.8	Ap. -0.05	Ap. -1	Ap. 55%	Cal. 1.89	Cal. 0.10
			-1.2	Ap. -0.45	Ap. -3	Ap. 64%	Cal. 6.60	Cal. 0.34
			-1.6	Ap. -0.85	Ap. -7	Ap. 73%	Cal. 17.55	Cal. 0.91
			-2.0	Ap. -1.25	Ap. -15	Ap. 80%	Cal. 41.21	Cal. 2.13
Ref. [3]	Microfluid GDE flow cell 0.5 ml/min Catholyte(pH = 2) CO_2 flow 50 mL/min	Pb/PtRu-GDL S_{geo}: 0.1 cm^2	2.5	Ap. -1.1	Ap. -20	Ap. 60%	Cal. 1.03	Cal. 0.75
			3	Ap. -1.35	Ap. -55	Ap. 93%	Cal. 4.39	Cal. 3.18
			3.5	Ap. -1.6	Ap. -150	Ap. 90%	Cal. 11.59	Cal. 8.40
			4	Ap. -1.9	Ap. -350	Ap. 92%	Cal. 27.64	Cal. 20.03
Ref. [4]	GDE flow cell 10ml/min 0.5M $NaHCO_3$, CO_2 flow 10ml/min.	Sn-GDE S_{geo}: 10.2 cm^2	——	-0.6	Ap. -3	Ap. 20%	Cal. 5.25	Cal. 0.19
			——	-0.8	Ap. -5	Ap. 55%	Cal. 24.08	Cal. 0.87
			——	-1.0	Ap. -10	Ap. 65%	Cal. 56.92	Cal. 2.06
			——	-1.2	Ap. -18	Ap. 60%	Cal. 94.57	Cal. 3.43
Ref. [5]	H-cell +GDE holder, 130 ml 0.1M Na_2SO_4, CO_2 flow 10ml/min	In/C-GDL S_{geo}: 0.95 cm^2	——	Ap. -1.2	-7.5	38%	Cal. 2.32	Cal. 0.38

Ref. [6]	2C cell, 10ml CO_2-bubbled 0.1 M $KHCO_3$, CO_2 flow 6 ml/min.	Hierarchical Cu pillar electrode S_{geo}: 1 cm^2	——	-0.2	Ap. -0.4	Ap. 9.5%	Cal. 0.03	Cal. 0.07
			——	-0.4	Ap. -0.9	Ap. 24%	Cal. 0.19	Cal. 0.40
			——	-0.6	Ap. -1.9	Ap. 26%	Cal. 0.42	Cal. 0.92
			——	-0.8	Ap. -3.4	Ap. 22%	Cal. 0.64	Cal. 1.40
			——	-1.0	Ap. -4.6	Ap. 18%	Cal. 0.71	Cal. 1.55
Ref. [7]	H-type cell, 75ml CO_2-bubbled 0.5 M $KHCO_3$, CO_2 flow not given	SnOx(100-8)/GDL S_{geo}: 4 cm^2	——	Ap. -1	-14	83.4%	Cal. 40.09	Cal. 11.62
Ref. [8]	GDE cell, 50ml 0.5M KHCO3 circulate CO_2 flow 30 ml/min.	Sn-NPs/GDL S_{geo}: 4 cm^2	Ap. -3.1	——	-10	Ap. 90%	Cal. 33.12	Cal. 14.4
Ref. [9]	H-type cell, 75ml CO_2-bubbled 0.5 M $KHCO_3$, (PH=7.4) CO_2 flow not given	SnOx@MWCNT-COOH on GDL S_{geo}: 4 cm^2	——	-0.95	Ap. -1.3	Ap. 50%	Cal. 2.23	Cal. 0.647
			——	-1.05	Ap. -3.0	Ap. 55%	Cal. 5.66	Cal. 1.642
			——	-1.15	Ap. -6.0	Ap. 70%	Cal. 14.42	Cal. 4.180
			——	-1.25	Ap. -9.3	Ap. 77%	Cal. 24.59	Cal. 7.128
			——	-1.35	Ap. -13.0	Ap. 60%	Cal. 26.78	Cal. 7.764
Ref. [10]	H-cell, 10ml CO_2-saturated 0.5M $NaHCO_3$ (pH 7.2), No CO_2 flow during eCO_2R	Hierarchical Mesoporous SnO2 Nanosheets on Carbon Cloth S_{geo}: 2 cm^2	——	Ap. -0.38	Ap. -2	Ap. 28%	Cal.	Cal. 2.09
			——	Ap. -0.58	Ap. -7	Ap. 35%	Cal. 4.21	Cal. 9.14
			——	Ap. -0.78	Ap. -24	Ap. 46%	Cal. 18.96	Cal. 41.21
			——	Ap. -0.98	Ap. -50	Ap. 90%	Cal. 77.27	Cal. 80
			——	Ap. -1.18	Ap. -70	Ap. 50%	Cal. 60.10	Cal. 130.64
Ref. [11]	H-cell, 30ml 1.0 M $KHCO_3$, CO_2 flow 20 ml/min.	SnO_2/carbon Aerogels "SnO_2/CA-80" S_{geo}: 2 cm^2	——	-0.55	Ap. -5	Ap. 37%	Ap. 12.14	Ap. 8.80
			——	-0.65	Ap. -10	Ap. 72%	Ap. 25.39	Ap. 18.40
			——	-0.75	Ap. -15	Ap. 71%	Ap. 25.39	Ap. 18.40
			——	-0.85	Ap. -25	Ap. 73%	Ap. 26.50	Ap. 19.20
			——	-0.95	Ap. -34	Ap. 75%	Ap. 27.05	Ap. 19.60
			——	-1.05	Ap. -44	Ap. 60%	Ap. 20.42	Ap. 14.80
			——	-1.15	Ap. -53	Ap. 44%	Ap. 15.46	Ap. 11.20

Ref. [12]	H-cell, 65 ml 0.5 M $KHCO_3$ CO_2 flow 30 ml/min	SnPb alloy on carbon cloth S_{geo}: 1 cm^2	——	Ap. -1.38	-57.3	79.8%	Cal. 39.26	Ap. 13
Ref. [13]	H-cell, 75 ml CO_2-saturated 0.5 M $KHCO_3$, No CO_2 flow during eCO_2R.	Cu-CDots nanocorals S_{geo}: 0.49 cm^2	——	-0.5	Ap. -1	Ap. 25%	Cal. 0.11	Cal. 0.03
			——	-0.6	Ap. -3.4	Ap. 50%	Cal. 0.72	Cal. 0.21
			——	-0.7	Ap. -6	Ap. 68%	Cal. 1.72	Cal. 0.50
			——	-0.8	Ap. -9.5	Ap. 58%	Cal. 2.32	Cal. 0.67
Ref. [14]	H-cell, Ap. 30 ml 0.1 M K_2HPO_4 / 0.1 KH_2PO_4 electrolyte (pH 6.7), No CO_2 flow during eCO_2R.	$Pt_xPd_{(100-x)}$ /C NPs S_{geo}: 0.49 cm^2	——	-0.1	Ap. -1.4	Ap. 20%	Cal. 0.19	Cal. 0.14
			——	-0.2	Ap. -1.6	Ap. 20%	Cal. 0.22	Cal. 0.16
			——	-0.3	Ap. -1.8	Ap. 70%	Cal. 0.85	Cal. 0.62
			——	-0.4	Ap. -2	Ap. 84%	Cal. 1.13	Cal. 0.82
			——	-0.5	Ap. -4	Ap. 60%	Cal. 1.62	Cal. 1.17
Ref. [15]	2C cell, AEM 8 ml 0.1 M $KHCO_3$, CO_2 flow 20 ml/min.	Sn foil S_{geo}: 4.5 cm^2	——	-0.4	Ap. -0.0195	Ap. 13%	Cal. 0.01	Cal. 0.03
			——	-0.6	Ap. -0.1365	Ap. 10%	Cal. 0.05	Cal. 0.14
			——	-0.87	Ap. -3	Ap. 67%	Cal. 7.77	Cal. 21.10
			——	-1.0	Ap. -7.3	Ap. 70%	Cal. 19.74	Cal. 53.64
			——	-1.27	Ap. 14.3	Ap. 54%	Cal. 29.83	Cal. 81.07

S_{geo}: electrode geometric surface area,
Ap.: Approximate value as seen directly from the given diagrams in literature,
Cal.: Calculated value based on the given and approximate values.
For the calculation method:
Hypothesis the current density *j* and fomate production rate held constant within 1 hour,

$$\text{formate yield per hour (mg/h)} = \frac{FE_{formate} \times Q \times M_{r(formate)}}{F \times 2} = \frac{FE_{formate} \times j \times S_{geo} \times 3600 \times 46}{96500 \times 2}$$

$$\text{formate conc. per hour (mM/h)} = \frac{formate\ yield\ per\ hour}{M_{r(formate)} \times Vol._{catholyte}}$$

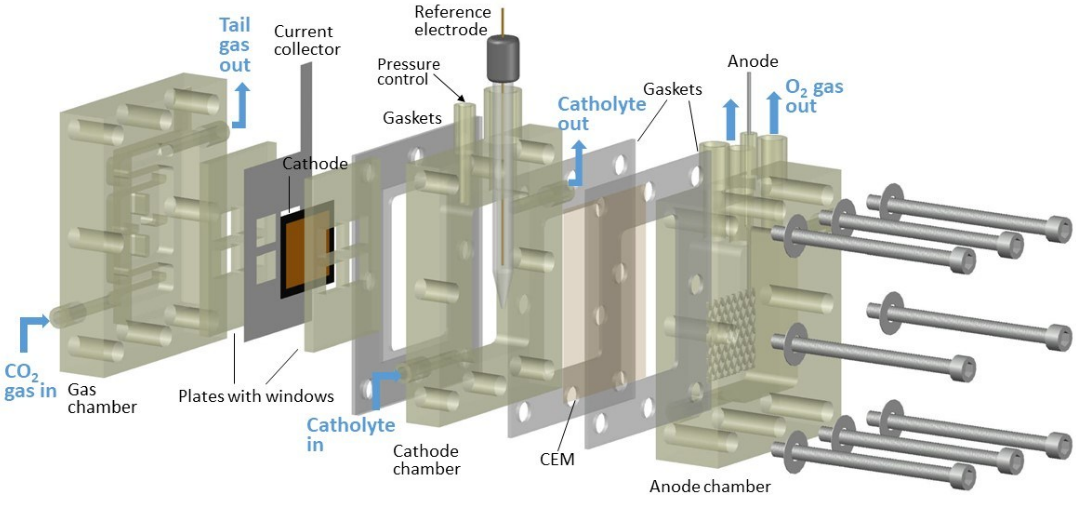

Figure S1 3D drawing of the GDE reactor set-up used in this study.

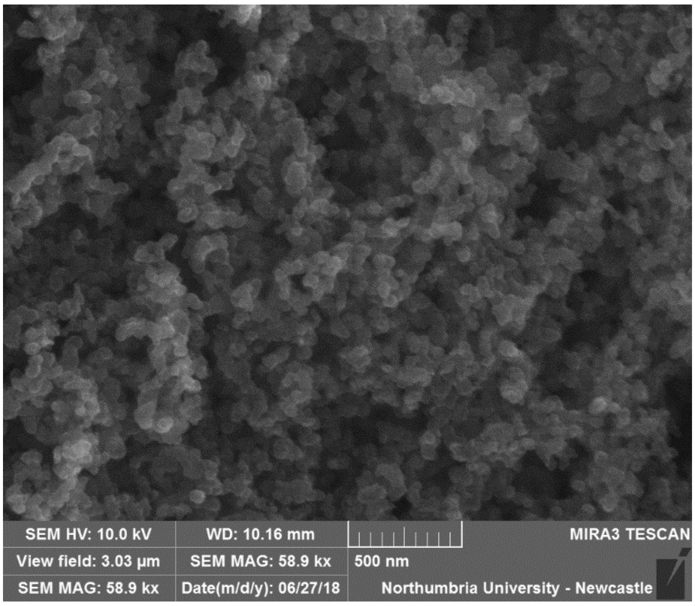

Figure S2 SEM images of Vulcan XC-72 carbon black.

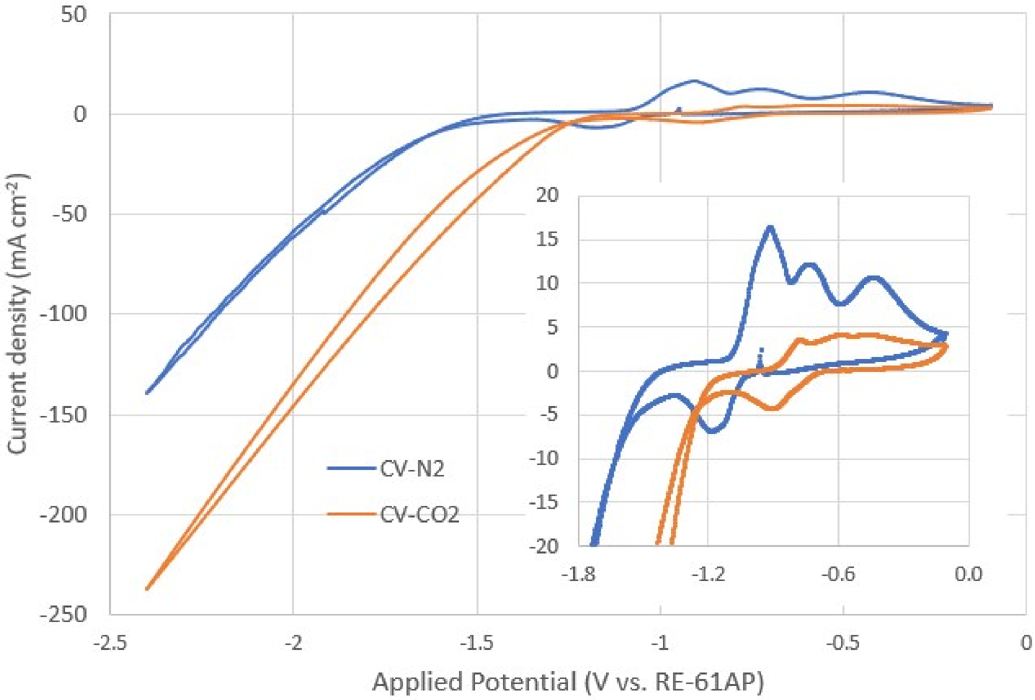

Figure S3 Cyclic voltammetry (CV) measurements under N_2 (blue) and CO_2 (orange) atmosphere using SnO_2/C(3.5) catalyst. Scan rate: 10 mV s^{-1}, scan circles: 3, both diagrams were taken from the 3rd cycle of scan.

Table S2 Normalized Faradaic efficiencies (FEs) of all the products and current density (*j*) of eCO$_2$Rs using different catalysts in gas diffusion electrode (GDE) cell with 1 M KOH catholyte, at wide range of cathodic potentials (V vs. RHE). Random error is shown in brackets.

Cathodic potential	Catalyst	FE (random error)			*j* (mA cm^{-2}) (random error)
		H_2	CO	$HCOO^-$	
-0.63 V	C	46.77% (3.95%)	12.39% (6.24%)	40.84% (10.19%)	-7.36 (1.97)
	SnO_2/C(0.5)	4.96% (0.97%)	33.77% (6.57%)	61.27% (7.54%)	-13.84 (6.23)
	SnO_2/C(1.0)	3.44% (1.27%)	31.38% (2.71%)	65.18% (1.44%)	-22.30 (3.68)
	SnO_2/C(3.5)	4.47% (2.24%)	17.11% (7.93%)	78.42% (5.69%)	-31.72 (2.10)
	SnO_2	17.09% (6.35%)	12.08% (10.05%)	70.83% (16.40%)	-28.20 (1.94)
-0.83 V	C	50.29% (3.62%)	15.82% (2.49%)	33.89% (1.13%)	-25.93 (2.16)
	SnO_2/C(0.5)	5.28% (1.09%)	34.03% (3.04%)	60.69% (4.13%)	-36.58 (0.30)
	SnO_2/C(1.0)	1.76% (4.08%)	27.42% (7.22%)	70.82% (3.14%)	-40.80 (10.08)
	SnO_2/C(3.5)	4.26% (0.87%)	18.35% (8.10%)	77.39% (7.23%)	-68.12 (0.28)
	SnO_2	15.54% (2.10%)	14.29% (10.32%)	70.17% (12.42%)	-44.56 (8.18)
-1.03 V	C	48.58% (1.13%)	18.99% (3.00%)	32.43% (4.13%)	-59.83 (9.20)
	SnO_2/C(0.5)	3.83% (1.06%)	20.28% (3.99%)	75.89% (2.93%)	-72.35 (2.62)
	SnO_2/C(1.0)	1.72% (2.67%)	22.25% (4.52%)	76.03% (1.85%)	-126.95 (6.64)
	SnO_2/C(3.5)	3.83% (1.17%)	18.44% (1.92%)	77.72% (0.74%)	-123.74 (4.08)
	SnO_2	21.40% (2.91%)	10.34% (5.59%)	68.26% (2.68%)	-106.63 (15.76)
-1.23 V	C	48.56% (6.71%)	25.19% (6.24%)	26.25% (0.47%)	-85.60 (3.11)
	SnO_2/C(0.5)	1.00% (1.29%)	25.18% (2.72%)	73.82% (1.43%)	-125.48 (24.15)
	SnO_2/C(1.0)	1.60% (2.44%)	17.51% (2.11%)	80.89% (4.55%)	-195.00 (5.73)
	SnO_2/C(3.5)	2.95% (1.02%)	16.71% (1.13%)	80.34% (2.15%)	-209.05 (13.11)
	SnO_2	23.81% (0.82%)	13.42% (1.13%)	62.77% (1.95%)	-174.05 (18.41)
-1.43 V	C	57.66% (1.51%)	19.87% (0.55%)	22.47% (2.06%)	-119.04 (6.85)

	SnO_2/C(0.5)	2.44% (0.59%)	14.29% (6.29%)	83.27% (6.88%)	-156.78 (23.64)
	SnO_2/C(1.0)	2.47% (1.41%)	16.18% (2.68%)	81.35% (4.09%)	-247.00 (8.94)
	SnO_2/C(3.5)	4.16% (0.04%)	11.51% (4.22%)	84.33% (4.18%)	-251.00 (8.43)
	SnO_2	37.55% (0.78%)	7.21% (1.18%)	55.24% (1.96%)	-235.11 (5.62)

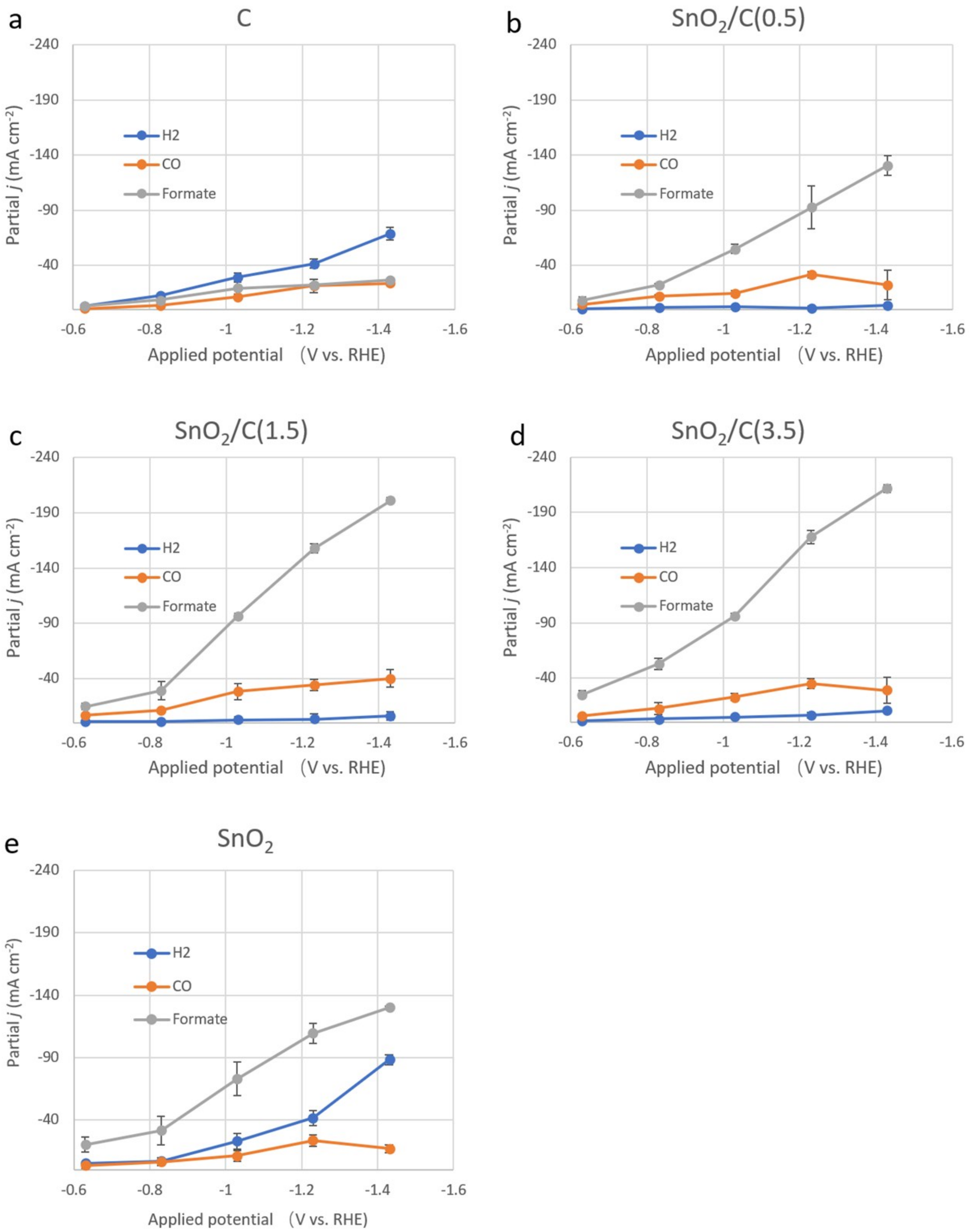

Figure S4 Partial current densities to produce H_2, CO, and format from eCO_2R as a function of the applied potential for different catalysts: a) C, b) SnO_2/C(0.5), c) SnO_2/C(1.5), d) SnO_2/C(3.5), e) SnO_2.

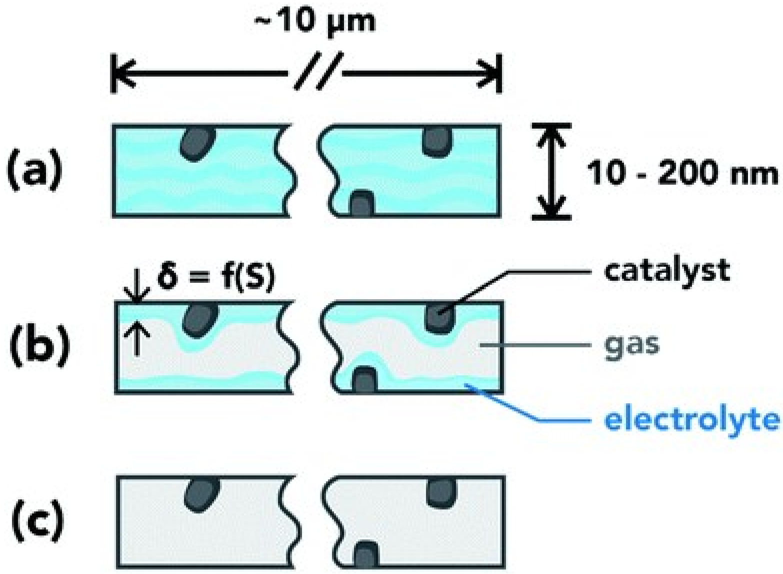

Figure S5 Schematic of pore conditions in the catalyst layer. (a) Flooded pore: pore volume filled with electrolyte. (b) Wetted pore: a thin layer of electrolyte covers the pore walls. (c) Dry pore: catalyst inactive due to lack of an ionic pathway. Reproduced from Ref. [16] with permission from the PCCP Owner Societies.

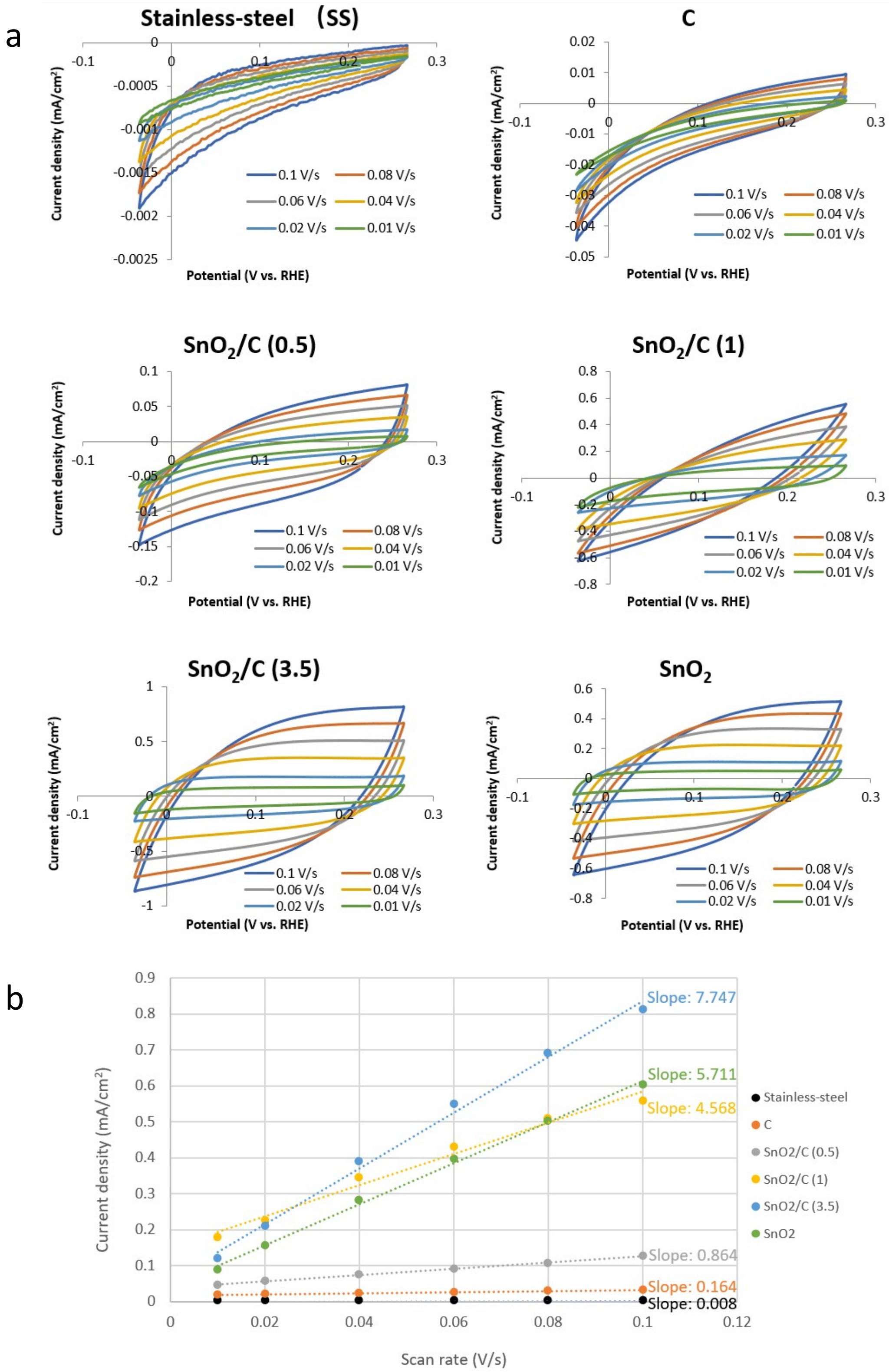

Figure S6 Determination of double-layer capacitance for a smooth stainless-steel sheet and the SnO_2/C-GDEs with various SnO_2/C mass ratio. a) CVs taken in the same electrochemical cell with a cation exchange membrane and 0.1 M $HClO_4$ electrolyte as reported before[17], over a range of scan rates in a potential window where only double-layer charging and discharging is relevant for stainless-steel and SnO_2/C-GDEs. b) Current due to double-layer charge/discharge plotted against CV scan rate for stainless-steel and SnO_2/C-GDEs.

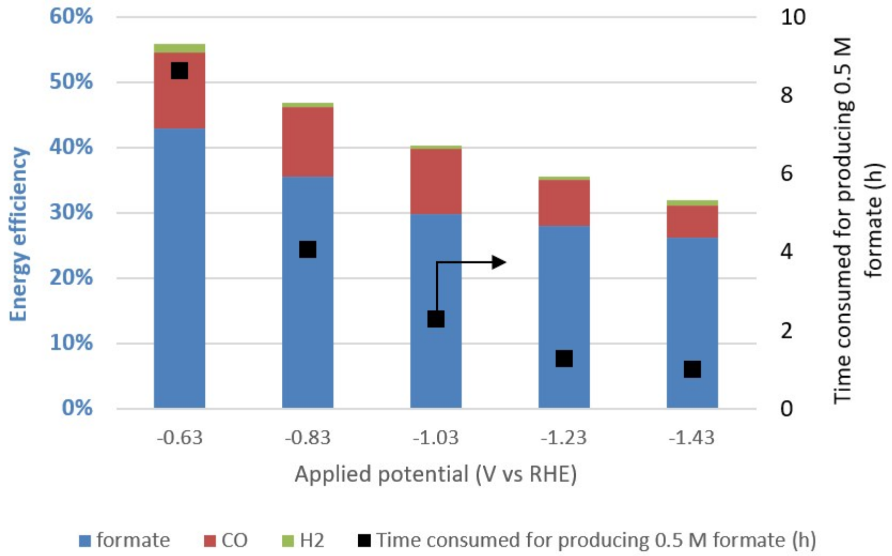

Figure S7 Energy efficiencies of all the products from eCO_2R and the time consumed for producing 0.5 M formate at at specific applied potentials -0.63 ~ -1.43 V with static catholyte.

Table S3 Calculations on half-cell reduction potentials (in reduction form) involved in formate fuel cell when formate concentration is 0.5 M at pH=14, 60 °C. Gibbs–Helmholtz equation, Nernst equation were used based on the database from Outokumpu HSC Chemistry 6.0 software.

Redox reactions	$\Delta H_r^\ominus$ (KJ)	$\Delta S_r^\ominus$ (J K^{-1})	$\Delta G_r^\ominus$ (KJ)	E^0 (V vs SHE)	E (V vs SHE)
Anode half-cell: $CO_2 + 2H_2O + 2e^- \rightarrow HCOOH + 2OH$	79.689	-343.01	181.96	-0.944	-0.954
Cathode half-cell $\frac{1}{2}O_2 + H_2O + 2e^- \rightarrow 2OH^-$	-174.22	-324.63	-77.43	+0.402	+0.402
Full-cell $HCOOH + \frac{1}{2}O_2 \rightarrow CO_2 + H_2O$	-253.91	18.39	-259.39	______	1.356

$\Delta G_r^\ominus = \Delta H_r^\ominus - T\Delta S_r^\ominus$ $E^0 = -\frac{\Delta G_r^\ominus}{zF}$ $E = E^0 + \frac{RT}{zF}\ln\frac{a_{Ox}}{a_{Red}}$	$\Delta H_r^\ominus$: change in enthalpy at standard state $\Delta S_r^\ominus$: change in entropy at standard state $\Delta G_r^\ominus$: change in the Gibbs free energy at standard state *E^0:* standard half-cell reduction potential *E:* half-cell reduction potential *z:* the number of electrons transferred in the half-cell reaction *F: Faradaic constant, 96485 C mol^{-1}.* *R:* gas constant, 8.413 *T: temperature, here is 298.15 K* a_{Ox}/a_{Red}: chemical activity of the oxidized/reduced form, for solid or pure phase, *a*=1; for ions in solution, *a* can be related to ion concentration.

References

1 Wang, Q., Dong, H. & Yu, H. Development of rolling tin gas diffusion electrode for carbon dioxide electrochemical reduction to produce formate in aqueous electrolyte. *Journal of Power Sources* **271**, 278-284 (2014).

2 Wu, J., Risalvato, F. G., Ma, S. & Zhou, X.-D. Electrochemical reduction of carbon dioxide III. The role of oxide layer thickness on the performance of Sn electrode in a full electrochemical cell. *J. Mater. Chem. A* **2**, 1647-1651 (2014).

3 Lu, X., Leung, D. Y., Wang, H. & Xuan, J. A high performance dual electrolyte microfluidic reactor for the utilization of CO2. *Applied energy* **194**, 549-559 (2017).

4 Irtem, E. *et al.* Low-energy formate production from CO 2 electroreduction using electrodeposited tin on GDE. *J. Mater. Chem. A* **4**, 13582-13588 (2016).

5 Bitar, Z., Fecant, A., Trela-Baudot, E., Chardon-Noblat, S. & Pasquier, D. Electrocatalytic reduction of carbon dioxide on indium coated gas diffusion electrodes—Comparison with indium foil. *Applied Catalysis B: Environmental* **189**, 172-180 (2016).

6 Chung, J., Koh, J., Kim, E.-H. & Woo, S. I. Hierarchical Cu pillar electrodes for electrochemical CO 2 reduction to formic acid with low overpotential. *Phys. Chem. Chem. Phys.* **18**, 6252-6258 (2016).

7 Li, Y. *et al.* Rational design and synthesis of SnOx electrocatalysts with coralline structure for highly improved aqueous CO2 reduction to formate. *ChemElectroChem* **3**, 1618-1628 (2016).

8 Lei, T. *et al.* Continuous electroreduction of carbon dioxide to formate on Tin nanoelectrode using alkaline membrane cell configuration in aqueous medium. *Catalysis Today* **318**, 32-38 (2018).

9 Zhang, Q. *et al.* Electrochemical Reduction of CO2 by SnOx Nanosheets Anchored on Multiwalled Carbon Nanotubes with Tunable Functional Groups. *ChemSusChem* **12**, 1443-1450 (2019).

10 Li, F., Chen, L., Knowles, G. P., MacFarlane, D. R. & Zhang, J. Hierarchical mesoporous SnO2 nanosheets on carbon cloth: a robust and flexible electrocatalyst for CO2 reduction with high efficiency and selectivity. *Angew. Chem., Int. Ed.* **56**, 505-509 (2017).

11 Yu, J., Liu, H., Song, S., Wang, Y. & Tsiakaras, P. Electrochemical reduction of carbon dioxide at nanostructured SnO2/carbon aerogels: The effect of tin oxide content on the catalytic activity and formate selectivity. *Appl. Catal., A* **545**, 159-166 (2017).

12 Choi, S. Y., Jeong, S. K., Kim, H. J., Baek, I.-H. & Park, K. T. Electrochemical reduction of carbon dioxide to formate on tin–lead alloys. *ACS Sustainable Chemistry & Engineering* **4**, 1311-1318 (2016).

13 Guo, S. *et al.* Cu-CDots nanocorals as electrocatalyst for highly efficient CO 2 reduction to formate. *Nanoscale* **9**, 298-304 (2017).

14 Kortlever, R., Peters, I., Koper, S. & Koper, M. T. Electrochemical CO2 reduction to formic acid at low overpotential and with high faradaic efficiency on carbon-supported bimetallic Pd–Pt nanoparticles. *ACS Catal.* **5**, 3916-3923 (2015).

15 Feaster, J. T. *et al.* Understanding selectivity for the electrochemical reduction of carbon dioxide to formic acid and carbon monoxide on metal electrodes. *ACS Catal.* **7**, 4822-4827 (2017).

16 Weng, L.-C., Bell, A. T. & Weber, A. Z. Modeling gas-diffusion electrodes for CO 2 reduction. *Phys. Chem. Chem. Phys.* **20**, 16973-16984 (2018).

17 Li, C. W. & Kanan, M. W. CO2 reduction at low overpotential on Cu electrodes resulting from the reduction of thick Cu2O films. *J. Am. Chem. Soc.* **134**, 7231-7234 (2012).